



In situ FTIR spectroscopic studies of (bi)sulfate adsorption on electrodes of Pt nanoparticles supported on different substrates

Dong-Mei Zeng, Yan-Xia Jiang, Zhi-You Zhou, Zhang-Fei Su, Shi-Gang Sun^{*,1}

State Key Laboratory of Physical Chemistry of Solid Surfaces, Department of Chemistry, College of Chemistry and Chemical Engineering, Xiamen University, Xiamen 361005, China

ARTICLE INFO

Article history:

Received 21 July 2009

Received in revised form 8 November 2009

Accepted 11 November 2009

Available online 4 December 2009

Keywords:

(Bi)sulfate

Adsorption

Pt nanoparticles

Anomalous IR property

In situ FTIRS

ABSTRACT

Nanostructured Pt electrodes were prepared by electrodeposition of Pt nanoparticles on different substrates (GC, Pt and Au) under cyclic voltammetric conditions and with various number (n) of potential cycling, and were denoted as nm-Pt/S(n) (S = GC, Pt and Au). Adsorption of (bi)sulfate on the nm-Pt/S(n) was studied by *in situ* FTIR reflection spectroscopy. It has been revealed that the nanostructured Pt electrodes exhibit anomalous IR properties for (bi)sulfate adsorption regardless of the different reflectivity of substrate, i.e. the IR absorption of (bi)sulfate species adsorbed on all the nm-Pt/S(n) electrodes is significantly enhanced and the IR band direction is completely inverted in comparison with the same species adsorbed on a bulk Pt electrode. The two IR bands around 1200 and 1110 cm^{-1} attributed to adsorbed (bi)sulfate species are shifted linearly with increasing electrode potential, yielding Stark tuning rates ($d\tilde{\nu}/dE_S$) of 152.1 and 21.1 $\text{cm}^{-1} \text{V}^{-1}$ on nm-Pt/GC(20), respectively. Along with increasing n , the Stark tuning rate of the IR band around 1200 cm^{-1} decreases quickly and declined to 7.6 $\text{cm}^{-1} \text{V}^{-1}$ on nm-Pt/GC(80), while the Stark tuning rate of the IR band near 1100 cm^{-1} is fluctuated between 23.0 and 16.2 $\text{cm}^{-1} \text{V}^{-1}$. It has determined that the enhancement of IR absorption of (bi)sulfate adsorbed on nanostructured Pt electrode is varied with substrate material and n , and a maximal 16-fold enhancement of the IR band near 1200 cm^{-1} has been measured on the nm-Pt/GC(30) electrode. The *in situ* FTIR studies illustrated that the adsorption of (bi)sulfate occurs mainly in the double layer potential region, and reaches a maximum around 0.80 V. The results demonstrated also that the competitive adsorption of CO and oxygen species can inhibit completely (bi)sulfate adsorption, which has evidenced a weak interaction of (bi)sulfate with nm-Pt/S(n) electrode surface.

© 2009 Elsevier Ltd. All rights reserved.

1. Introduction

Nanomaterials exhibit peculiar properties due to their nano-size effects, surface effects, quantum optics effects, etc., and display potential applications in electronics [1], optics [2], catalysis [3], magnetic data storage [4], and so on. Investigation of the IR peculiar properties is of importance to reveal the fundamental aspects of nanomaterials. The optical properties of nanomaterials were extensively studied in recent years by using vibration spectroscopy, such as the surface-enhanced Raman scattering (SERS) [5], surface-enhanced IR absorption spectroscopy (SEIRAS) [6], surface-enhanced second harmonic generation (SESHG) [7] and surface-enhanced sum frequency generation (SESEFG) [8]. The former two optical properties are considered to arise from the size and separation of surface nanoscale islands, while the latter two optical

properties are strongly dependent on the structure of nanomaterials.

It has been reported that the electrocatalysts of metal nanomaterials exhibit, in general, anomalous infrared property [9–17], which consists in the inversion of the direction of IR band of adsorbates (anomalous absorption), the enhancement of IR absorption and the broadening of IR band width (inhomogeneous broadening) in comparison with the same species adsorbed on a corresponding bulk metal surface. Previous studies concerning the anomalous IR property of nanomaterials were conducted mostly by using CO adsorption as a probe molecule. It is known that the CO adsorption on transition metals leads to the formation of a 5σ bond together with a $d-\pi^*$ back donation [18], which results in a strong interaction. Besides, IR absorption of CO species appears around 2100–1800 cm^{-1} region depending on their coordination mode to surface, i.e. the highest IR energy region provided by modern FTIR instruments. Such high IR energy gives rise to almost the most sensitive spectral response in the mid-infrared range [19,20]. It is worthwhile to investigate the anomalous IR property of nanomaterials using weak adsorbates such as (bi)sulfate species as probes

* Corresponding author. Tel.: +86 592 2180181; fax: +86 592 2183047.

E-mail address: sgsun@xmu.edu.cn (S.-G. Sun).

¹ ISE member.

that yield IR absorption in the fingerprint region (1500–800 cm⁻¹), where most organic fuel molecules give rise to characteristic IR absorption. It may be expected that such investigation may provide essential significances in three aspects: (1) to explore the anomalous IR property of nanomaterials in different conditions other than those in previous studies employed probe molecules that yielded a strong interaction with electrode surface [9–17]; (2) to study the adsorptive behaviors of sulfuric acid, which is the most widely used electrolyte in electrochemical systems, on nanostructured Pt electrodes; and (3) to extend the anomalous IR property of nanomaterials in studies of electrocatalysis of direct organic molecule fuel cells, because nanomaterials such as Pt or Pt alloy nanoparticles supported on carbon are widely used electrocatalysts, and the anomalous IR features of the inversion of IR band direction and the enhancement of IR absorption are very useful in determining intermediates and products involved in oxidation reaction of organic fuel molecules.

Extensive studies have been done so far concerning (bi)sulfate adsorption on electrode surface, mostly on noble metals, such as Pt [21–43], and Au [44], and the investigations of (bi)sulfate are mostly focused on bulk metal electrodes. The studies have demonstrated that the (bi)sulfate adsorption can affect drastically electrochemical reactions of methanol oxidation [45], H₂ oxidation [45], O₂ reduction [46], CO₂ reduction [47], coadsorption of water [48,49], and the underpotential deposition (UPD) of Cu [50], etc. Numerous methods have been used in past decades to investigate the adsorption of (bi)sulfate on metal electrodes, among them infrared spectroscopy has provided the most important information about adsorbates of (bi)sulfate at molecule level [22–29,34–41]. As the infrared bands of adsorbed (bi)sulfate on a bulk metal surface and those of solution (bi)sulfate species appear in the same direction and at similar wavenumbers in IR spectra, it is difficult to discern the IR bands arising from adsorbed (bi)sulfate, which leads to the complication of assigning the adsorbed (bi)sulfate species and of understanding the adsorptive behaviors of (bi)sulfate. Undoubtedly, further study of (bi)sulfate on surface of nonmaterial electrodes would be very significant in order to reveal the adsorptive properties of sulfuric acid electrolyte at molecule level, if nanostructured electrodes also exhibit anomalous infrared property for such weakly adsorbed species.

The present paper has put emphasis upon the behaviors of (bi)sulfate adsorption on Pt nonmaterial electrodes. Nanostructured Pt electrodes were prepared by electrodeposition of Pt nanoparticles on different substrates under cyclic voltammetric conditions. *In situ* FTIR spectroscopy was employed to investigate (bi)sulfate adsorption on the nanostructured Pt electrodes. The results demonstrated that, for the first time, the nanostructured Pt electrodes exhibit also anomalous IR property for weakly adsorbed (bi)sulfate species that yield IR absorption in fingerprint region, at which the IR energy is much lower than that in the 2000 cm⁻¹ region. The *in situ* FTIR studies illustrated that the adsorption of (bi)sulfate occurs mainly in the double layer potential region on nanostructured Pt electrodes, and reaches a maximum around 0.80 V.

2. Experimental

Nanostructured Pt electrodes were prepared through electrodeposition of Pt nanoparticles on different substrates (glassy carbon (GC), Pt and Au of 5 mm in diameter). The deposition was carried out in 0.002 M K₂PtCl₆ + 0.1 M H₂SO₄ solution under cyclic voltammetric conditions, in which the electrode potential was cycled between -0.25 V and 0.40 V (vs. SCE, 0.05–0.70 V (RHE)) at a scan rate 0.05 V s⁻¹. The size and density of deposited Pt nanoparticles depend on the numbers (*n*) of potential cycles applied in elec-

trodeposition. Nanostructured Pt electrodes prepared on different substrates and with various *n* are denoted hereafter as nm-Pt/S(*n*), where S stands for substrate of GC, Pt or Au, respectively. The substrate was sealed into a Teflon holder and polished mechanically using sand paper (6#) and alumina powder of size 5, 1 and 0.3 μm, then cleaned in an ultrasonic bath, and finally subjected to potential cycling at 0.10 V s⁻¹ in 0.1 M H₂SO₄ solution to remove possible impurity on the surface before Pt nanoparticles deposition. The surface structure of the as-prepared electrode was characterized by scanning electron microscopy (SEM) on a LEO-1530 electron microscopy.

All solutions were prepared with super pure H₂SO₄ and Millipore water (18 MΩ cm) supplied from a Milli-Q lab apparatus (Nihon Millipore Ltd.). The solutions were deaerated by bubbling N₂ before measurement. A saturated calomel electrode (SCE) was used as reference electrode, and a platinized platinum foil was served as counter electrode. In order to facilitate the comparison of results of this paper with those reported in the literatures [21–44], the electrode potentials recorded versus the SCE were first converted into the reversible hydrogen electrode (RHE) scale, and then presented in this paper. A 263 potentiostat/galvanostat (EG&G) was used to control the potential of electrode. All measurements were carried out at room temperature.

Electrochemical *in situ* FTIR reflection spectroscopy measurements were conducted on a Nexus 870 spectrometer equipped with a liquid-nitrogen-cooled MCT-A detector. A CaF₂ disk was used as IR window. A thin layer configuration was approached by pushing the electrode against the IR window during FTIR measurements. The incident IR beam was aligned at about 60° to the normal of electrode surface.

In situ FTIR spectra were collected using SNIFTIRS (subtractively normalized interfacial FTIR spectroscopy) procedure [22–29,34–41]. The result spectra were reported as the relative change in reflectivity and calculated as follows:

$$\frac{\Delta R}{R} = \frac{R(E_S) - R(E_R)}{R(E_R)} \quad (1)$$

where $R(E_S)$ and $R(E_R)$ are single-beam spectra of reflection collected at sample potential E_S and reference potential E_R , respectively. Each single-beam spectrum was co-added with 1000 interferograms at a spectral resolution of 8 cm⁻¹. As in the SNIFTIRS procedure, the collection of interferograms was done alternatively at E_S and E_R . In order to study clearly the IR features of (bi)sulfate adsorbates, an appropriate E_R is crucial. We have compared a series of E_R and found that a maximal intensity of IR bands of adsorbed (bi)sulfate can be obtained when the E_R is set at 0.24 V (see details in Fig. 5). So the 0.24 V was used as reference potential throughout all *in situ* FTIR studies of (bi)sulfate adsorption on nanostructured Pt electrodes, which coincides with the literatures [30–32] that at such low potential almost no anions are adsorbed on Pt electrode surface.

3. Results and discussion

3.1. Cyclic voltammetric (CV) studies and SEM characterization

A stable cyclic voltammogram (CV) of nm-Pt/GC(*n*) electrode in 0.1 M H₂SO₄ is shown in Fig. 1a. The potential scan range includes three regions, i.e. hydrogen region (0.03–0.40 V), double layer region (0.40–0.75 V) and oxygen region (0.75–1.55 V). Fig. 1a is similar to the cyclic voltammogram of a bulk Pt electrode [31]. We observe two pairs of hydrogen adsorption/desorption current peaks around 0.12 and 0.18 V in the hydrogen region, respectively. In the positive-going potential scan (PGPS), oxygen adsorption current appears in the oxygen region as a broad peak from 0.75 to 1.17 V and follows a plateau; and in the negative-going potential

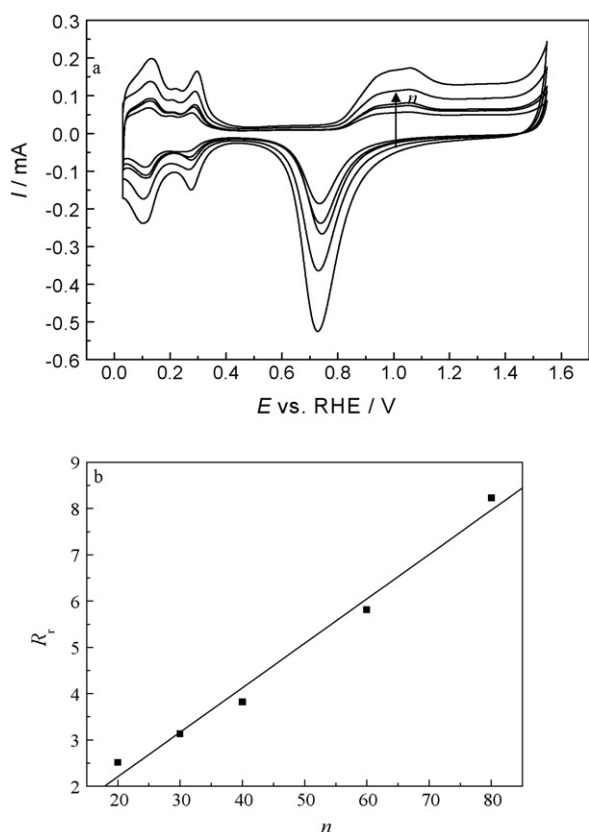


Fig. 1. (a) Cyclic voltammograms of nm-Pt/GC(*n*) electrode in 0.1 M H₂SO₄, potential scan rate: 0.05 V s⁻¹; (b) relationship between *R_r* and *n*.

scan (NGPS) a reduction current peak is observed near 0.74 V. The amplitude of all these current peaks increases with the increase of *n*. Cyclic voltammograms recorded on an nm-Pt/Pt(*n*) and an nm-Pt/Au(*n*) display similar features. While in the case of nm-Pt/Au(*n*) electrodes an additional reduction current peak is observed near 1.17 V in the NGPS, which is attributed to the oxide reduction of Au substrate. The appearance of this current peak due to the reduction of surface Au oxide indicates that the nanostructured Pt film is so porous (as seen in SEM images below) that the Au substrate can be oxidized at high electrode potentials. It is worthwhile to note that no faraday current except the current of double layer charging is determined in the double layer region.

As a matter of fact, a polished Pt electrode will always have a roughness higher than 1. In the present study, a roughness of ca. 2.0 has been measured from the ratio of electro-active surface area to geometrical surface area. The electro-active surface area is calculated by $Q_H/210 \mu\text{C cm}^{-2}$, where Q_H is the hydrogen adsorption charge measured by integration of the CV curve of the polished Pt electrode, and the value $210 \mu\text{C cm}^{-2}$ is taken for adsorption of a monolayer of hydrogen on a smooth polycrystalline Pt electrode [31]. To normalize the adsorption surface sites of the nm-Pt/S(*n*) referring to the polished Pt, we define the relative roughness (*R_r*) of the nm-Pt/S(*n*) electrodes by comparing the electro-active area of nm-Pt/S(*n*) electrodes with that of the polished Pt electrode, i.e.

$$R_r = \frac{A(\text{nm-Pt/S}(n))}{A(\text{Pt})} = \frac{Q_H(\text{nm-Pt/S}(n))}{Q_H(\text{Pt})} \quad (2)$$

where $A(\text{nm-Pt/S}(n))$ and $A(\text{Pt})$ are electro-active surface area of nm-Pt/S(*n*) and polished Pt electrodes, respectively, $Q_H(\text{nm-Pt/S}(n))$ and $Q_H(\text{Pt})$ are the electric charge of hydrogen adsorption that were measured by integration of corresponding CV curves in the hydrogen region.

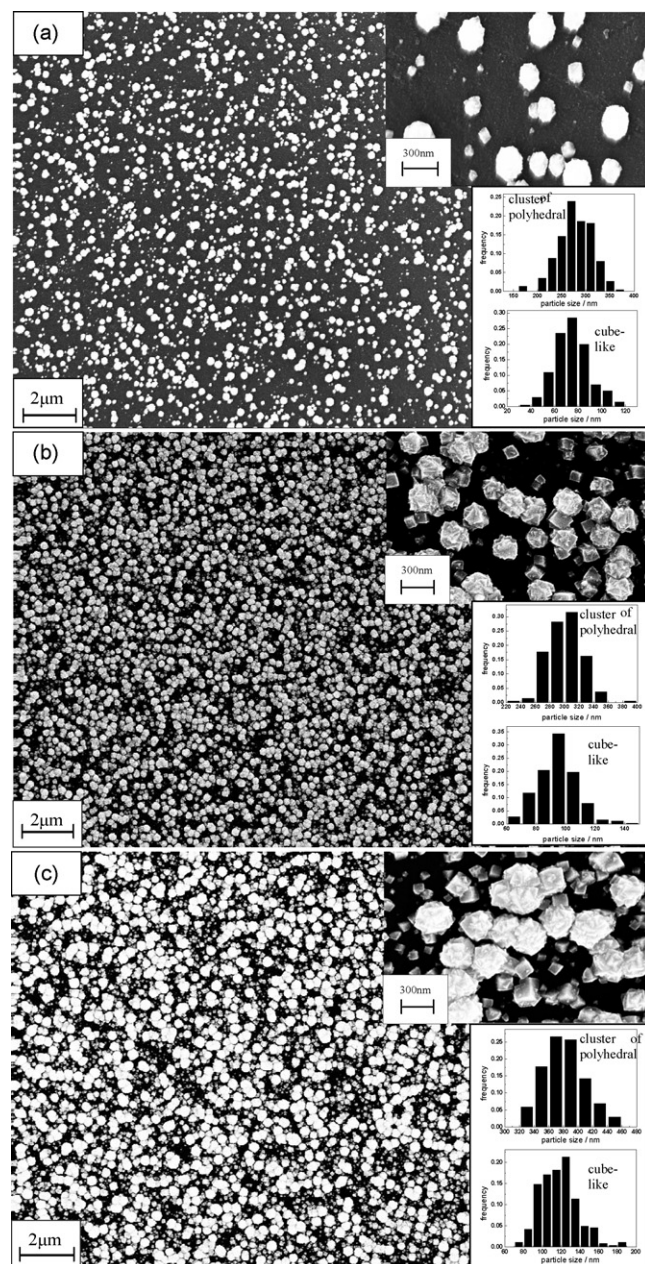


Fig. 2. SEM images of (a) nm-Pt/GC(20), (b) nm-Pt/GC(40) and (c) nm-Pt/GC(80) electrodes, the inserts are the corresponding size histograms of Pt nanoparticles of different structure: congeries of polyhedral particles and cube-like particles.

The relationship between *R_r* and *n* acquired with nm-Pt/GC(*n*) electrodes is plotted in Fig. 1b. It illustrates clearly a linear variation of *R_r* with *n*. Such linear relationship between *R_r* and *n* is also maintained for nm-Pt/Pt(*n*) and nm-Pt/Au(*n*) electrodes.

The SEM images in Fig. 2 illustrate that the nm-Pt/GC(*n*) electrodes are composed of Pt nanoparticles dispersed on GC substrate. These Pt nanoparticles may be classified into two categories, i.e. cube-like particles and congeries of polyhedra as seen clearly in the insert to Fig. 2b. Along with increasing *n* from 20 (Fig. 2a) to 80 (Fig. 2c), the density of Pt nanoparticles on the substrate significantly increases, and the size of both type nanoparticles is also enlarged. As indicated by histograms in Fig. 2a, when *n* = 20, the average dimension of the congeries of polyhedra is 277 ± 34 nm, and the average size of the cube-like particles is 75 ± 15 nm; when *n* = 40, the average dimension of the congeries of polyhedra increases to 301 ± 23 nm (Fig. 2b), and the average size

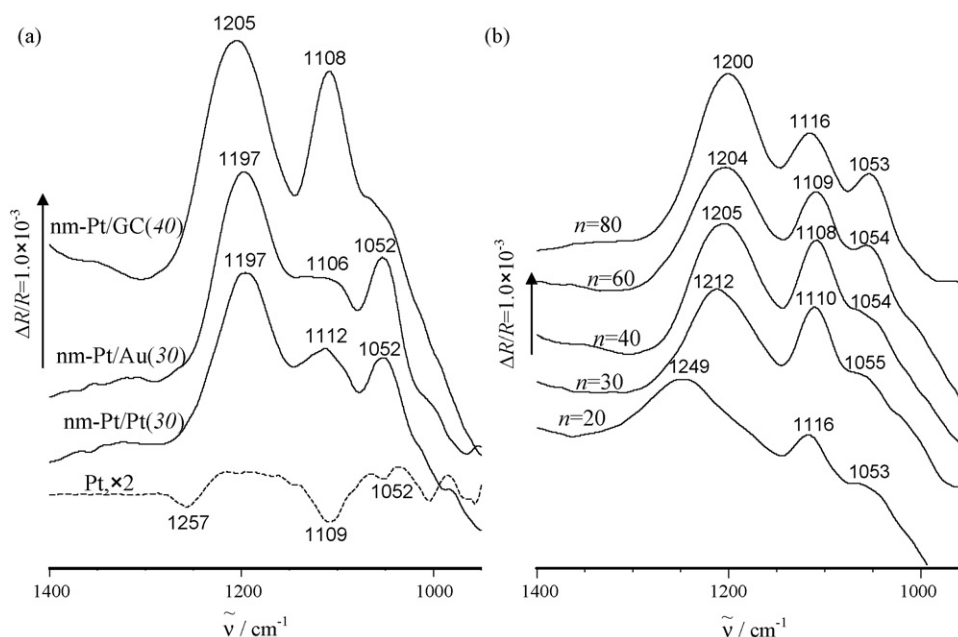


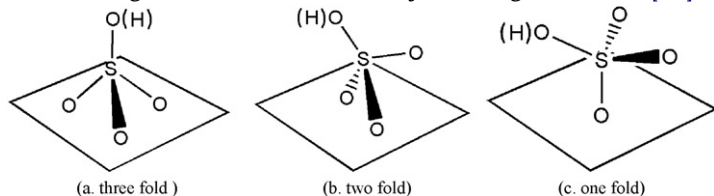
Fig. 3. (a) *In situ* SNIFTIR spectra of (bi)sulfate adsorbed on a bulk Pt (dash line, 2000 scans, $E_R = 0.05$ V, the y-scale is multiplied by a factor 2 in order to illustrate clearly the comparison) and nm-Pt/S(n) electrodes (1000 scans, $E_R = 0.24$ V), 0.1 M H_2SO_4 , $E_S = 0.75$ V, 8 cm^{-1} ; (b) *In situ* SNIFTIR spectra of (bi)sulfate adsorbed on nm-Pt/GC(n) electrodes with n varying from 20 to 80, $E_R = 0.24$ V, $E_S = 0.75$ V, 0.1 M H_2SO_4 , 1000 scans, 8 cm^{-1} .

of the cube-like particles is augmented to 95 ± 13 nm (Fig. 2b); as n increases further to 80, the average dimension of the congeries of polyhedra increases further to 381 ± 28 nm (Fig. 2c), and the average size of the cube-like particles reaches 118 ± 20 nm (Fig. 2c).

3.2. *In situ* FTIR spectroscopic studies

3.2.1. Comparison of adsorption behaviors of (bi)sulfate on a bulk Pt and nanostructured Pt electrodes

The comparison of IR features of (bi)sulfate adsorbed on nanostructured Pt electrodes and on a bulk Pt electrode in 0.1 M H_2SO_4 is presented in Fig. 3. In order to facilitate the comparison, electrodes of Pt nanoparticles deposited on different substrates with close R_f were used, i.e. nm-Pt/GC(40) ($R_f = 3.8$), nm-Pt/Pt(30) ($R_f = 4.2$) and nm-Pt/Au(30) ($R_f = 4.4$). It is known that the (bi)sulfate adsorption on electrode surface may occur in three configurations, i.e. the threefold, twofold and one-fold configurations, as illustrated by the diagram below [23].



From spectra in Fig. 3, we observe three negative-going bands around 1257, 1109 and 1052 cm^{-1} in spectrum recorded of the bulk Pt electrode, corresponding to IR absorption at E_S . Although extensive studies were presented in the literature, the assignment of these bands is still not clear. These IR bands have been attributed to IR absorption of sulfate [24,25,37], bisulfate [26,38,39], or both species [41]. As these IR bands correspond to IR absorption of adsorbed species derived from sulfuric acid, they are commonly assigned to (bi)sulfate species as described in recent literatures [28,29,33,40]. We adopted this assignment in the present paper. Hoshi et al. [29] assigned the band around 1257 cm^{-1} to the coordinated S–O stretching of threefold adsorbed (bi)sulfate species, and the band near 1109 cm^{-1} to the S–O stretching of the coordi-

nated twofold adsorbed (bi)sulfate, while Nart et al. [25] attributed the band at 1052 cm^{-1} to the coordinated S–O vibration of onefold species.

In comparison with those IR features appeared in the spectrum of the bulk Pt electrode, anomalous IR features are observed clearly in spectra of (bi)sulfate adsorbed on nm-Pt/S(n) electrodes, consisting mainly in four aspects: (1) the IR bands become positive-going, i.e. the anomalous IR absorption, indicating that these bands are derived from the adsorbed (bi)sulfate species. This has been confirmed also by the linear shift of band center with E_S (see details in Fig. 5). In case of bulk Pt electrode, the IR bands of adsorbed (bi)sulfate and those of (bi)sulfate in solution are the same direction of negative-going in spectra, which arose difficulty in discerning whether these IR bands to adsorbed or to solution (bi)sulfate species. Nevertheless the inversion of the direction of IR bands in spectra recorded on nanomaterials is very helpful to confirm the adsorption status of species [15]; (2) the IR band observed at 1257 cm^{-1} on bulk Pt is red-shifted to 1205 cm^{-1} on nm-Pt/S(n); (3) the IR band appears clearly at 1052 cm^{-1} in spectra of both nm-Pt/Pt(30) and nm-Pt/Au(30) electrodes, while it becomes a shoulder peak in the spectrum of nm-Pt/GC(40) electrode; and (4) the intensity of IR bands especially that of the band around 1200 cm^{-1} has been significantly enhanced. We can see clearly that these anomalous IR characters are all presented in spectra of the nm-Pt/S(n) electrodes regardless of the different substrate materials (GC, Pt and Au) that bear different chemical nature and different reflectivity, although slight differences in IR features may be noticed. This result has demonstrated undoubtedly that the anomalous IR property is a peculiar character of the nanostructured Pt film.

Fig. 3b illustrates the variation of IR features of (bi)sulfate adsorbed on nm-Pt/GC(n) electrodes in 0.1 M H_2SO_4 at $E_S = 0.75$ V. Along with increasing n , the band around 1200 cm^{-1} is red-shifted, while the band near 1110 cm^{-1} remains almost at similar wavenumbers. At first, the band close to 1054 cm^{-1} is a shoulder peak in contrast to the strong bands around 1200 and 1110 cm^{-1} , then becomes more pronounced in spectra recorded on both nm-Pt/GC(60) and nm-Pt/GC(80) electrodes. This band does not shift with the increase of n .

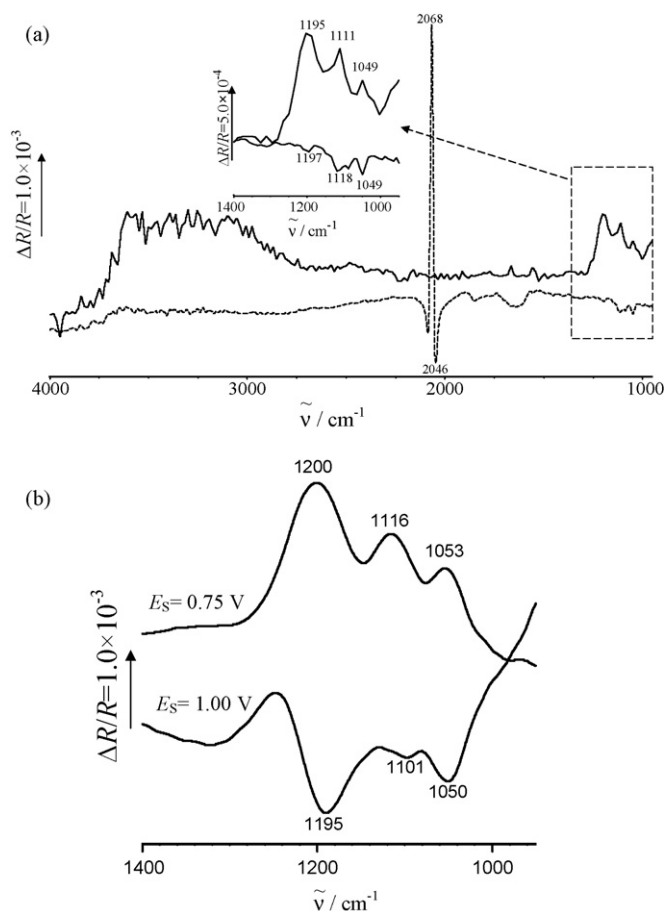


Fig. 4. (a) *In situ* SNIFTIR spectra of (bi)sulfate adsorbed on nm-Pt/GC(80) electrode with CO adsorbed on electrode surface (dash line, 6000 scans, $E_R = 0.10 \text{ V}$) and after stripping completely the adsorbed CO_{ad} (solid line, 1000 scans, $E_R = 0.24 \text{ V}$), $0.1 \text{ M H}_2\text{SO}_4$, $E_S = 0.40 \text{ V}$, 16 cm^{-1} . (b) *In situ* SNIFTIR spectra recorded on nm-Pt/GC(80) with E_S respectively at 0.75 V (double layer potential region) and at 1.00 V (oxygen potential region), $0.1 \text{ M H}_2\text{SO}_4$, $E_R = 0.24 \text{ V}$, 1000 scans, 8 cm^{-1} .

3.2.2. The competitive adsorption of (bi)sulfate with CO and oxygen species

In order to study further the competition adsorption behaviors of (bi)sulfate, CO adsorption at low potentials and oxygen adsorption at high potentials were introduced. The comparison of *in situ* FTIR spectra before and after the oxidation of a saturation layer of CO pre-adsorbed on nm-Pt/GC(80) electrode is illustrated in Fig. 4a. When a saturation layer CO is pre-adsorbed on nm-Pt/GC(80) electrode, we observe from the spectrum (the dashed line) a strong IR band around 2060 cm^{-1} that is assigned to IR absorption of CO adsorbed on nanostructured Pt electrode surface. The distortion of this band confirms the anomalous IR property of the nm-Pt/GC(80) for CO adsorption as reported previously for CO adsorption on nanostructured Pt electrodes [13]. As the adsorbed CO exists at both E_R (0.10 V) and E_S (0.40 V) [13] and its bonding with Pt surface is so strong that it could desorb any other adsorbates, all the bands corresponding to (bi)sulfate (1197 , 1118 and 1049 cm^{-1}) are negative-going, which evidences that these IR bands arise from IR absorption of solution (bi)sulfate species that were diffused at E_S from the bulk solution into the thin layer between electrode and IR window due to electrostatic effect, and evidences that no adsorbed (bi)sulfate species are presented on the CO covered nm-Pt/GC(80) electrode surface. However, when the saturation layer of pre-adsorbed CO is removed completely by stripping it at a high electrode potential, i.e. 1.00 V in the present experiment, the IR features of (bi)sulfate are changed dramatically. As can be seen

from the spectrum (the solid line) recorded with $E_R = 0.24 \text{ V}$ and $E_S = 0.40 \text{ V}$ after stripping completely the pre-adsorbed CO on the nm-Pt/GC(80) electrode surface, the CO band disappears and the three bands around 1197 , 1118 and 1049 cm^{-1} all become positive-going and with enhanced intensity, confirming that the (bi)sulfate species are re-adsorbed on the nm-Pt/GC(80) electrode surface. This result has indicated also that the adsorption of CO is much stronger than that of (bi)sulfate species on the nm-Pt/GC(80) electrode surface. Moreover, both adsorbed CO and (bi)sulfate on nanostructured Pt electrodes give rise to anomalous IR features.

We have compared also the IR features of spectrum recorded at a potential ($E_S = 0.75 \text{ V}$) in the double layer region with that acquired at a potential ($E_S = 1.00 \text{ V}$) in the oxygen region, the results obtained on a nm-Pt/GC(80) electrode are displayed in Fig. 4b. It can be seen that the three IR bands around 1200 , 1100 and 1050 cm^{-1} in spectrum of E_S setting at the oxygen region (1.00 V) are all negative-going, predicating that the (bi)sulfate species are in solution, while these bands in the spectrum recorded with $E_S = 0.75 \text{ V}$ are turned into positive-going with enhanced intensity. This result may be interpreted as follows: in the oxygen region, oxygen can adsorb on nm-Pt/GC(80) surface to form platinum oxide species such as Pt(OH), PtO, Pt(OH)₃, PtO₂ [51], which can desorb the adsorbed (bi)sulfate or inhibit the (bi)sulfate anions adsorption on the one hand, and on the other hand, the anions diffused from bulk solution into in the thin layer between electrode and IR window increase significantly as potential rising [34–36]. The large quantity of anions gathered in the thin layer has resulted strong IR bands of solution (bi)sulfate species, which can be also observed in the spectrum recorded on a bulk Pt electrode at the same E_S , for which no anomalous IR property of the bulk Pt electrode for (bi)sulfate adsorption. In the spectra recorded on a bulk Pt electrode, the IR bands are always negative-going regardless of $E_S = 0.75 \text{ V}$ or $E_S = 1.0 \text{ V}$. It is obvious that, from these results, the adsorption of (bi)sulfate species is weaker than that of oxygen species on Pt electrode surface.

3.2.3. Effects of electrode potential on (bi)sulfate adsorption

In order to study the behaviors of potential dependence of (bi)sulfate adsorption, an appropriate reference potential E_R in the SNIFTIRS studies is important. In the past study, the potential of 0.05 V was chosen as the reference potential on bulk and single crystal Pt electrodes [21–44], since radioactive tracer measurements showed negligible adsorption of anions at this potential [52]. Fig. 5 shown *in situ* FTIR spectra recorded with $E_S = 0.75 \text{ V}$ and E_R varying from 0.05 to 0.30 V (solid line). It can be seen that the IR bands of (bi)sulfate adsorbed on nanostructured Pt surface, i.e. the bands near 1205 and 1108 cm^{-1} , have reached the largest intensity with E_R at 0.24 V . This result indicates that the adsorbed (bi)sulfate adsorbed on nanostructured Pt surface at 0.24 V presents a minimum among all other E_R studied. As the result *in situ* FTIR spectra were reported as the relative change in reflectivity, the less adsorbed (bi)sulfate at E_R will make clearer the IR features of adsorbed (bi)sulfate at E_S . So 0.24 V was set up as E_R in the present *in situ* FTIR study of (bi)sulfate adsorption on nm-Pt/S(*n*) electrodes. In comparison, 0.05 V and 0.24 V were also used as E_R for *in situ* FTIR study of (bi)sulfate adsorption on a bulk Pt electrode (see the dashed line in Fig. 5). The intensity of IR bands of adsorbed (bi)sulfate on bulk Pt surface reached a maximum value with $E_R = 0.05 \text{ V}$, which is in consistence with the literature [52].

By setting up $E_R = 0.24 \text{ V}$, a series of *in situ* FTIR spectra were recorded on the nm-Pt/GC(40) electrode and displayed in Fig. 6a. These spectra illustrate the potential dependence of IR features of adsorbed (bi)sulfate. Two obvious positive-going bands appear respectively around 1180 and 1110 cm^{-1} at 0.30 V , and shifted positively and linearly with increasing E_S . The Stark tuning rate is measured from the slope of the linear variation of band center ($\tilde{\nu}$) with E_S , and values of 57.3 and $18.7 \text{ cm}^{-1} \text{ V}^{-1}$ were evaluated

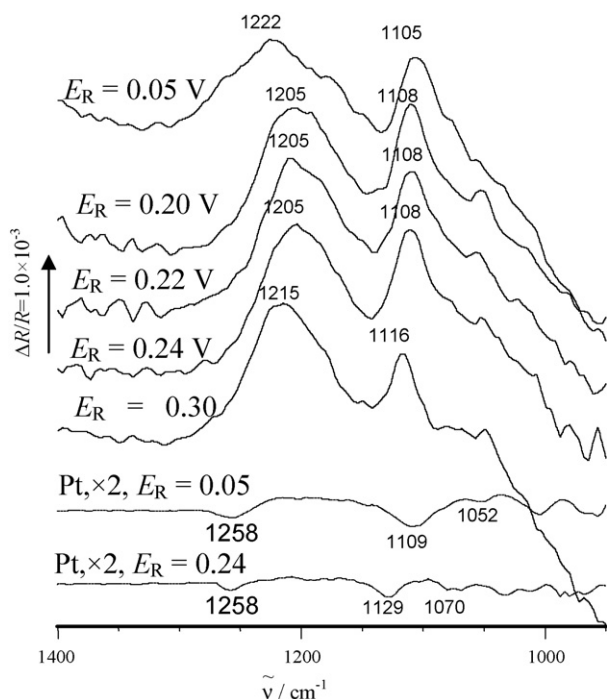


Fig. 5. *In situ* SNIPTIR spectra of (bi)sulfate adsorbed on (a) nm-Pt/GC(40) (solid line, 1000 scans) and (b) a bulk Pt electrodes (dash line, 2000 scans, the y-scale is multiplied by a factor 2 in order to illustrate clearly the comparison) with different E_R in hydrogen potential region, 0.1 M H_2SO_4 , $E_S = 0.75$ V, 8 cm^{-1} .

from Fig. 6b for the two bands, respectively. It is interesting to note that the Stark tuning rates of these two IR bands vary in different ways with n . The increase in n causes a significant decrease in $d\tilde{\nu}/dE_S$ of the band around 1200 cm^{-1} . As listed in Table 1, the Stark tuning rate of the band around 1200 cm^{-1} decreases quickly with increasing n . The $d\tilde{\nu}/dE_S$ of this band is 152.1 $cm^{-1} V^{-1}$ for $n = 20$,

Table 1
Variation of Stark tuning rates ($d\tilde{\nu}/dE_S$) with n measured on nm-Pt/GC(n).

n	$d\tilde{\nu}/dE_S$ ($cm^{-1} V^{-1}$) (1200 cm^{-1})	$d\tilde{\nu}/dE_S$ ($cm^{-1} V^{-1}$) (1100 cm^{-1})
20	152.1	21.1
30	86.4	19.6
40	57.3	18.7
60	37.5	23.0
80	7.6	16.2

but it is decreased to 7.6 $cm^{-1} V^{-1}$ when n is 80. The decrease in Stark tuning rate has been observed also with the increase of R_f for CO adsorbed on nanostructured Pt electrodes [14]. As the R_f increases almost linearly with increasing n (see Fig. 1b), the rapid decrease in Stark tuning rate of the band around 1200 cm^{-1} is certainly an effect of surface structure. In contrast, only a small fluctuation of $d\tilde{\nu}/dE_S$ between 23.0 and 16.2 $cm^{-1} V^{-1}$ was measured for the band around 1110 cm^{-1} . It is known that the Stark tuning rate of the IR band of (bi)sulfate is also related to the adsorbed geometry [23–25]. A (bi)sulfate adsorbed with threefold geometry (ca. 1200 cm^{-1}) yields a $d\tilde{\nu}/dE_S$ about 100 $cm^{-1} V^{-1}$ on Pt(1 1 1) [23,24,26,27], while a twofold geometry (bi)sulfate gives rise to smaller $d\tilde{\nu}/dE_S$ of 12.5 $cm^{-1} V^{-1}$ for the coordinated S–O band (ca. 1100 cm^{-1}) [25]. The larger $d\tilde{\nu}/dE_S$ of the band at ca. 1200 cm^{-1} of adsorbed (bi)sulfate has been interpreted by a back donation of electron from metal to LUMO orbit of the (bi)sulfate [23], and the integrated effects of the consequence of the electric field on the effective dipole moments and the coverage [25].

The difference of the coverage does not cause substantial discrepancy of the $d\tilde{\nu}/dE_S$ between the threefold and the twofold (bi)sulfate species, since the estimated $d\tilde{\nu}/dE_S$ of the singleton threefold (bi)sulfate is still bigger than that of the twofold one [24,29]. When n increases, the R_f also increases, while the $d\tilde{\nu}/dE_S$ of the band near 1200 cm^{-1} decreases obviously. As illustrated by Fig. 2, the density of Pt nanoparticles on GC substrate increases along with increasing n (particles per μm^2 : nm-Pt/GC(20): 2 (cube-like), 4 (congeries of polyhedral); nm-Pt/GC(40): 9 (cube-like), 5

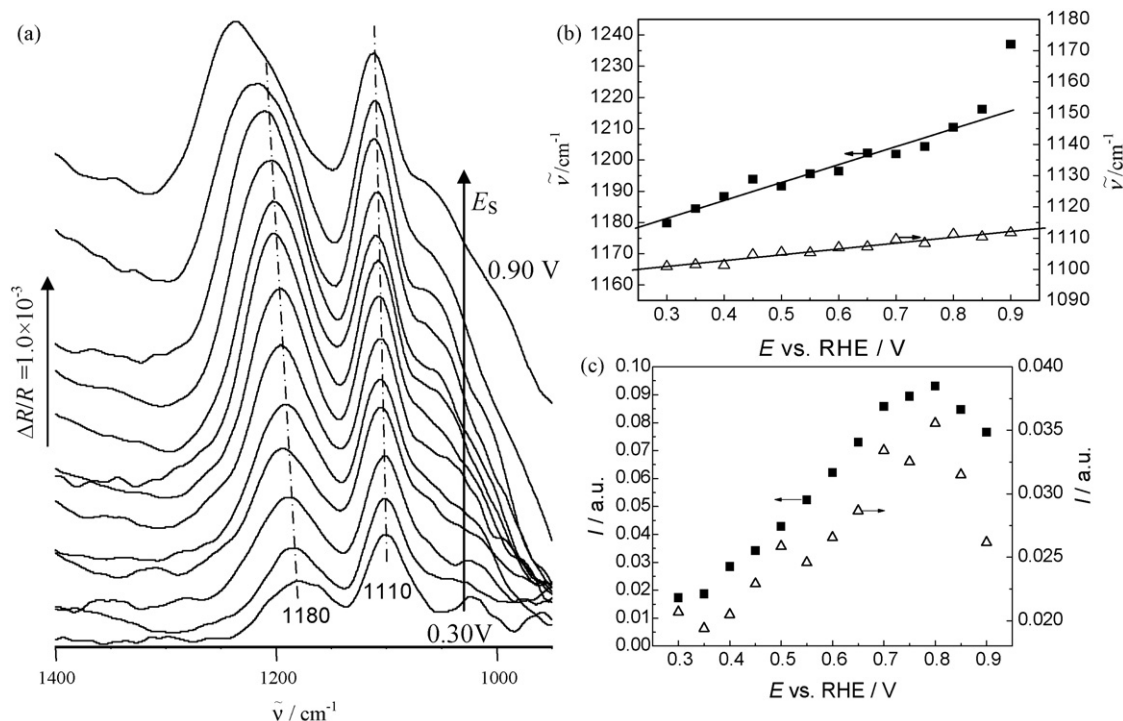


Fig. 6. (a) *In situ* SNIPTIR spectra of (bi)sulfate adsorbed on nm-Pt/GC(40), the corresponding potential dependences of (b) the center and (c) the intensity of the IR bands near 1200 cm^{-1} (■) and 1100 cm^{-1} (△). 0.1 M H_2SO_4 , 8 cm^{-1} , 1000 scans, $E_R = 0.24$ V, E_S varying progressively from 0.30 to 0.90 V with an interval of 0.05 V.

(congeries of polyhedral); nm-Pt/GC(80): 18 (cube-like), 6 (congeries of polyhedral)). As a result of the mechanical renormalization [53] and the Pauli repulsion [54], the multicoordination to the surface causes a blue shift of the band center [25,38], and the more coordination between (bi)sulfate and the electrode surface, the more sensitive the adsorbed (bi)sulfate to the surface structure. The trend for the coordinated group frequencies is $\tilde{\nu}_{(S-O, \text{threefold})} > \tilde{\nu}_{(S-O, \text{twofold})} > \tilde{\nu}_{(S-O, \text{onefold})}$, i.e. $\tilde{\nu}_{(a)} > \tilde{\nu}_{(b)} > \tilde{\nu}_{(c)}$. Furthermore, the large variation of the Stark tuning rate is also dependent on the sensitivity of adsorptive modes to surface structures. The threefold mode is more sensitive to surface structure than the twofold mode does. As a consequence, the above results may confirm that the IR bands near 1200, 1100 and 1050 cm^{-1} could be assigned respectively to the S–O vibration of the coordinated threefold (bi)sulfate, twofold and onefold adsorbed (bi)sulfate species.

The variations of intensity (I) of the IR bands around 1200 and 1110 cm^{-1} are plotted versus potential in Fig. 6c. It can be seen that I of both bands increases almost linearly with increasing E_S and reaches a maximum at 0.80 V, then decreases with further increase of E_S beyond 0.80 V. We have tested that all nm-Pt/S(n) electrodes have yielded almost the similar variation, i.e. the intensity of IR bands of (bi)sulfate adsorption on all nm-Pt/S(n) electrodes achieves the maximal value at 0.80 V. The result implies that the adsorption of (bi)sulfate occurs mainly in the double layer potential region. This phenomenon is coincident with the thermodynamic studies of (bi)sulfate adsorption on Pt electrodes (Pt(hkl)), especially for Pt(111) [30,32,33], in which a maximal adsorption has been determined at 0.80 V (vs. RHE) as well.

3.2.4. The enhancement of IR absorption of (bi)sulfate adsorbed on nanostructured Pt electrodes

To study quantitatively the enhancement of IR absorption, an enhancement factor (Δ_{IR}) is designated to represent the degree of enhancement of IR absorption by (bi)sulfate adsorbed on nanostructured Pt electrodes referring to that on a bulk Pt electrode, i.e.

$$\Delta_{\text{IR}} = \frac{1}{R_r} \frac{I_{\text{IR}}(\text{nm-Pt/S}(n))}{I_{\text{IR}}(\text{Pt})} \quad (4)$$

where $I_{\text{IR}}(\text{nm-Pt/S}(n))$ and $I_{\text{IR}}(\text{Pt})$ are the integral IR band intensities of (bi)sulfate adsorbed on nm-Pt/S(n) and bulk Pt electrodes, respectively. R_r is the corresponding relative roughness of the nm-Pt/S(n) electrode evaluated by using Eq. (2), which is used to normalize the surface adsorption sites of nm-Pt/S(n) referring to a polished Pt electrode. The $I_{\text{IR}}(\text{nm-Pt/S}(n))$ is measured in the spectra collected at 0.75 V, since this potential is close to the potential at which the maximal intensity of IR bands of (bi)sulfate adsorbed on nm-Pt/S(n) is measured.

Table 2 lists the Δ_{IR} measured on nm-Pt/GC(n) electrodes. It can be seen that the Δ_{IR} depends on the number of cycles applied to electrodeposition of Pt nanoparticles on GC substrate. It is evident that the Δ_{IR} of the band near 1200 cm^{-1} ($\Delta_{\text{IR}}(1200 \text{ cm}^{-1})$) is much larger than the Δ_{IR} of the band around 1100 cm^{-1} ($\Delta_{\text{IR}}(1100 \text{ cm}^{-1})$), and the enhancement factor of both IR bands reaches a maximum when n is 30. The largest Δ_{IR} (1200 cm^{-1}) is 16.0 and the Δ_{IR} (1100 cm^{-1}) is only 3.7. On the nm-Pt/Pt(n) and nm-Pt/Au(n) electrodes, the largest Δ_{IR} values were also measured

at $n = 30$. The largest values of Δ_{IR} (1200 cm^{-1}) are respectively 9.0 and 9.1 on nm-Pt/Pt(30) and nm-Pt/Au(30), while the largest values of Δ_{IR} (1100 cm^{-1}) are only 2.0 and 1.7 on nm-Pt/Pt(30) and nm-Pt/Au(30). It is worthwhile noting that the GC substrate yields the largest enhancement of IR absorption among the three substrates used, illustrating the substrate effect on the IR features, which may be ascribed to the much lower reflectivity of the GC substrate than that of the Pt and Au metallic substrates. However, for thicker layers the IR enhancement depends mostly on the size, shape and distribution of the metal particles, which should be largely independent of the nature of the substrate.

Zheng and Sun [10] have investigated the adsorption of CO on nanostructured Ru film electrodes (nm-Ru/GC), and they found that the variation of the enhancement factor Δ_{IR} versus the film thickness is manifested an asymmetrical volcano curve; the maximum value appears when the film thickness is 86 nm. Heaps and Griffiths [55] have also illustrated the IR intensity of SAMs of PNTF formed on gold films, and they observed that the IR intensity did not always increase with film thickness, there is also a maximum at a certain film thickness. In the current study, the thickness of nanoparticles film definitely increases with n , so the variation of Δ_{IR} with n is certainly related to the variation of thickness of film of Pt nanoparticles on substrates.

4. Conclusions

In the present paper, nanostructured Pt electrodes were prepared through electrodeposition of Pt nanoparticles on different substrates by applying cyclic voltammetry. Adsorption of (bi)sulfate on as-prepared nm-Pt/S(n) ($S = \text{GC, Pt and Au}$) and a bulk Pt electrodes was studied using *in situ* infrared reflection spectroscopy. An IR band around 1257 cm^{-1} in the spectra recorded on bulk Pt is assigned to IR absorption of S–O stretching of adsorbed threefold anions, while it has been shifted negatively to around 1200 cm^{-1} on nanostructured Pt electrodes. Other two IR bands around 1110 and 1050 cm^{-1} on bulk Pt are attributed to IR absorption of coordinated S–O vibration of the adsorbed twofold anions and onefold anions, respectively. Similar wavenumbers of these two bands were measured in spectra recorded on nanostructured Pt electrodes. Anomalous IR features were observed from *in situ* FTIR spectra of (bi)sulfate adsorption on all nanostructured Pt electrodes prepared in the current study, i.e. the IR absorption of (bi)sulfate species adsorbed on all the nm-Pt/S(n) electrodes is significantly enhanced and the IR band direction is completely inverted, in comparison with the same species adsorbed on a bulk Pt electrode. These anomalous IR features were attributed to the anomalous IR property of Pt nanoparticles film. Although the different substrates, which present different chemical nature and different reflectivity, yield different enhancement factors, the inversion of IR band direction for adsorbed (bi)sulfate is always maintained in spectra recorded on Pt nanoparticles film deposited on different substrates. This is the first demonstration that nanostructured Pt electrodes exhibit anomalous IR property for weakly adsorbed (bi)sulfate species, and also a first observation of anomalous IR features in the fingerprint region. It has found that the S–O stretching frequencies and the band intensities increase linearly with electrode potential in double layer region and reaches a maximum at 0.80 V, indicating a potential dependence of (bi)sulfate adsorption on nanostructured Pt electrodes. It has demonstrated also that the adsorbed (bi)sulfate can be desorbed by the adsorption of oxygen species with electrode potentials in the oxygen region, which is evidenced by the change of the direction of (bi)sulfate IR bands from positive-going ($E_S = 0.75 \text{ V}$, anomalous IR absorption of adsorbates) to negative-going ($E_S = 1.0 \text{ V}$, IR absorption of solution species that were diffused from bulk solution into the thin layer between electrode and IR win-

Table 2
Variation of Δ_{IR} with n measured on nm-Pt/GC(n).

	$\Delta_{\text{IR}}(1200 \text{ cm}^{-1})$	$\Delta_{\text{IR}}(1100 \text{ cm}^{-1})$
20	15.3	1.4
30	16.0	3.7
40	12.3	1.9
60	8.4	1.1
80	9.7	1.9

dow). The facts that both CO and oxygen adsorptions can inhibit the adsorption of (bi)sulfate anions confirmed the weak adsorption of (bi)sulfate anions on nanostructured Pt electrodes.

The current paper has demonstrated clearly the behaviors of (bi)sulfate adsorption on nanostructured Pt electrodes, and revealed also the anomalous IR property of nanostructured Pt for weak adsorbates. The study has extended the study of anomalous IR property of nanostructured electrodes from strongly adsorbed species to weakly adsorbed anions, and also from the highest energy region (2100–1800 cm⁻¹) provided by a modern FTIR instrument to fingerprint region, i.e. the relatively lower IR energy region where most organic fuel molecules give rise to characteristic IR absorption. The results revealed further that the anomalous IR properties are essential for nanostructured electrodes, and contributed to the understanding of the origin of peculiar property of nanomaterials as well. The anomalous IR features, i.e. the enhancement of IR absorption and the inversion of IR band direction, are significant for determining adsorbates including anions at molecule level, and for investigations of surface processes and reaction mechanism involved in electrocatalysis of direct organic molecule fuel cells that employ mainly Pt nanoparticles deposited on carbon materials as catalysts.

Acknowledgment

This study was supported by grants from National Natural Science foundation of China (Grant Nos. 20833005, 20873116 and 20828005).

References

- [1] V. Palermo, M. Palma, P. Samori, *Adv. Mater.* 18 (2006) 145.
- [2] V.M. Shalaev, A.K. Sarychev, *Phys. Rev. B* 57 (1998) 13265.
- [3] T.P. St. Clair, D.W. Goodman, *Top. Catal.* 13 (2000) 5.
- [4] L. Krusin-Elbaum, T. Shibauchi, B. Argyle, L. Gignac, D. Weller, *Nature* 410 (2001) 444.
- [5] R. Emory, W.E. Haskins, S. Nie, *J. Am. Chem. Soc.* 120 (1998) 8009.
- [6] M. Osawa, in: S. Kawata (Ed.), *Near-field Optics and Surface Plasmon Polaritons*, vol. 81, Springer-Verlag, Berlin, Germany, 2001, p. 163.
- [7] T.A. Leskova, M. Leyva-Lucero, E.R. Mendez, A.A. Maradudin, I.V. Novikov, *Opt. Commun.* 183 (2000) 529.
- [8] S. Baldelli, A.S. Epple, E. Anderson, *J. Chem. Phys.* 113 (2000) 5432.
- [9] G.Q. Lu, S.G. Sun, L.R. Cai, S.P. Chen, Z.W. Tian, K.K. Shiu, *Langmuir* 16 (2000) 778.
- [10] M.S. Zheng, S.G. Sun, *J. Electroanal. Chem.* 500 (2001) 223.
- [11] H. Gong, S.G. Sun, J.T. Li, Y.J. Chen, S.P. Chen, *Electrochim. Acta* 48 (2003) 2933.
- [12] H.C. Wang, S.G. Sun, J.W. Yan, H.Z. Yang, Z.Y. Zhou, *J. Phys. Chem. B* 109 (2005) 4309.
- [13] Q.S. Chen, S.G. Sun, J.W. Yan, J.T. Li, Z.Y. Zhou, *Langmuir* 22 (2006) 10575.
- [14] H. Gong, S.G. Sun, Y.J. Chen, S.P. Chen, *J. Phys. Chem. B* 108 (2004) 11575.
- [15] A.E. Bjerke, P.R. Griffiths, *Anal. Chem.* 71 (1999) 1967.
- [16] S. Park, Y.Y. Tong, A. Wieckowski, M.J. Weaver, *Electrochem. Commun.* 3 (2001) 509.
- [17] G. Orozco, C. Gutierrez, *J. Electroanal. Chem.* 484 (2000) 64.
- [18] G. Blyholder, *J. Phys. Chem.* 68 (1964) 2772.
- [19] H. Buijs, in: P.R. Griffiths, J.M. Chalmers (Eds.), *Handbook of Vibrational Spectroscopy*, John Wiley & Sons Ltd, Chichester, 2002.
- [20] E. Theodorou, J.R. Birch, in: P.R. Griffiths, J.M. Chalmers (Eds.), *Handbook of Vibrational Spectroscopy*, John Wiley & Sons Ltd, Chichester, 2002.
- [21] J. Clavilier, *J. Electroanal. Chem.* 107 (1980) 211.
- [22] K. Kunitatsu, M.G. Samant, H. Seki, *J. Electroanal. Chem.* 258 (1989) 163.
- [23] P.W. Faguy, N. Markovic, R.R. Adzic, C.A. Fierro, E.B. Yeager, *J. Electroanal. Chem.* 289 (1990) 245.
- [24] F.C. Nart, T. Iwasita, M. Weber, *Electrochim. Acta* 39 (1994) 961.
- [25] F.C. Nart, T. Iwasita, M. Weber, *Electrochim. Acta* 39 (1994) 2093.
- [26] P.W. Faguy, N.S. Marinkovic, R.R. Adzic, *Langmuir* 12 (1996) 243.
- [27] Y. Shingaya, M. Ito, *Chem. Phys. Lett.* 256 (1996) 438.
- [28] V. Climen, N. Garcia-Araez, J.M. Feliu, *Electrochem. Commun.* 8 (2006) 1577.
- [29] N. Hoshi, A. Sakurada, S. Nakamura, S. Teruya, O. Koga, Y. Hori, *J. Phys. Chem. B* 106 (2002) 1985.
- [30] J. Mostany, E. Herrero, J.M. Feliu, J. Lipkowski, *J. Phys. Chem. B* 106 (2002) 12787.
- [31] M.C. Santos, D.W. Miwa, S.A.S. Machado, *Electrochem. Commun.* 2 (2000) 692.
- [32] W. Savich, S.G. Sun, J. Lipkowski, A. Wieckowski, *J. Electroanal. Chem.* 388 (1995) 233.
- [33] N. Garcia-Araez, V. Climent, P. Rodriguez, J.M. Feliu, *Electrochim. Acta* 53 (2008) 6793.
- [34] M. Futamata, L.Q. Luo, C. Nishihara, *Surf. Sci.* 590 (2005) 196.
- [35] Y. Shingaya, K. Hirota, H. Ogasawara, M. Ito, *J. Electroanal. Chem.* 409 (1996) 103.
- [36] K. Hirota, M.B. Song, M. Ito, *Chem. Phys. Lett.* 250 (1996) 335.
- [37] G.J. Edens, X. Gao, M.J. Weaver, *J. Electroanal. Chem.* 375 (1994) 357.
- [38] Y. Shingaya, M. Ito, *J. Electroanal. Chem.* 467 (1999) 299.
- [39] A. Lachenwitzer, N. Li, J. Lipkowski, *J. Electroanal. Chem.* 532 (2002) 85.
- [40] K. Kunitatsu, T. Senzakib, G. Samjeske, M. Tsushima, M. Osawa, *Electrochim. Acta* 52 (2007) 5715.
- [41] F.C. Nart, T. Iwasita, *J. Electroanal. Chem.* 322 (1992) 289.
- [42] I. Fromondi, D. Scherson, *J. Phys. Chem. C* 111 (2007) 10154.
- [43] A. Kolics, A. Wieckowski, *J. Phys. Chem. B* 105 (2001) 2588.
- [44] K. Sato, S. Yoshimoto, J. Inukai, K. Itaya, *Electrochem. Commun.* 8 (2006) 725.
- [45] H. Kita, Y. Gao, T. Nakato, H. Hattori, *J. Electroanal. Chem.* 373 (1994) 177.
- [46] H. Kita, Y. Gao, K. Ohnishi, *Chem. Lett.* 23 (1994) 73.
- [47] N. Hoshi, T. Suzuki, Y. Hori, *J. Electroanal. Chem.* 416 (1996) 61.
- [48] M. Nakamura, H. Kato, N. Hoshi, *J. Phys. Chem. C* 112 (2008) 9458.
- [49] T. Kondo, J. Morita, K. Hanaoka, S. Takakusagi, K. Tamura, M. Takahashi, J. Mizuki, K. Uosaki, *J. Phys. Chem. C* 111 (2007) 13197.
- [50] K. Ataka, G. Nishina, W.B. Cai, S.G. Sun, M. Osawa, *Electrochem. Commun.* 2 (2000) 417.
- [51] N.H. Li, S.G. Sun, S.P. Chen, *J. Electroanal. Chem.* 430 (1997) 57.
- [52] G. Horanyi, J. Solt, F. Nagy, *J. Electroanal. Chem.* 31 (1971) 95.
- [53] T.B. Grimley, *Proc. Phys. Soc.* 79 (1962) 1203.
- [54] P.S. Bagus, W. Muller, *Chem. Phys. Lett.* 115 (1985) 540.
- [55] D.A. Heaps, P.R. Griffiths, *Vibrational Spectrosc.* 42 (2006) 45.